Jurnal Teknologi

Full Paper

CRACKING PATTERN ANALYSIS OF THE TURNING BAND METHOD (TBM) APPLICATION ON A SINGLE-REINFORCEMENT BAR CONCRETE BEAM MODELLING USING THE MAZARS DAMAGE

Nuraziz Handika*, Audiyati Ishmata Hani'a

Department of Civil Engineering, Faculty of Engineering, Universitas Indonesia, 16424, Depok, West Java, Indonesia

Article history
Received
19 December 2023
Received in revised form
17 April 2024
Accepted
17 April 2024
Published Online
17 October 202

*Corresponding author
n.handika@ui.ac.id

Graphical abstract

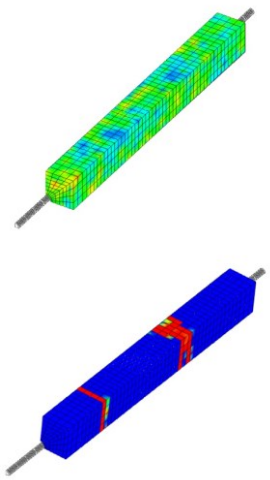

Abstract

The development of crack patterns in reinforced concrete structures is a randomly stochastic process influenced by the heterogeneous nature of concrete materials, which impacts the sensitivity to damage and variability in mechanical properties. The numerical simulation of damage pattern appearance on the reinforced concrete for special building structures needs a realistic result, especially in terms of crack distribution. The Turning Band Method (TBM) serves as a tool for assessing the variability of concrete heterogeneity, functioning as an operator to generate a random variable for each specific field. In this study, the investigation of crack patterns in reinforced concrete structures involves using a simple concrete beam sample, measuring 10x10x50 cm^3, with a single longitudinal reinforcement cast in the centre. This beam is subjected to an axial tensile loading, while the Mazar Damage Model is employed as the concrete behaviour law. Through the implementation of The Turning Band Method (TBM) and the variation of the random field parameters, distinct crack patterns are observed, not only the number but also the locations of cracks. The use of a smaller correlation length showed 2 cracks while the larger size had around 1 to 3 cracks, with the first crack localizations of each sample generally occurring in the middle surface, in which a noticeable contrast to non-TBM modelling just displays 1 crack. Furthermore, the resulting probability of cracks for ten random draws demonstrates similarity to experimental tests and numerical simulation of the previous study, both at global and local levels.

Keywords: Heterogeneity, Random Field, Turning Band Method, Mazar Damage Model, Crack Pattern

1.0 INTRODUCTION

Effective crack control is crucial for preserving the serviceability, durability, and sustainability of reinforced concrete structures throughout their service life [1]. As structures experience various types of damage over time, the mechanism driving the damage process in concrete structures impact their conditions and integrity. Therefore, detecting damage, which can lead to further crack propagation, is essential for ensuring structural safety [2].

Extensive research related to controlling and evaluating cracks has been done by adopting some methods from the visual investigation using the Cyclic Load Test (CLT) method and Acoustic Emission (AE) evaluation method [2], to the strengthening techniques involving the use of Carbon Fiber Reinforced Plastic (CFRP) sheets [3, 4]. Retrofitting methods employing CFRP sheet wrapping enhance the structural performance of cracked beam [3] and increase shear resistance [4]. While these methods are mainly able and useful in determining and retrofitting damage process in reinforced concrete beams, however, it remains some improvements for an accurate analytical results [2]. This condition emphasizes the necessity for more comprehensive research to control and quantify the concrete

damage, particularly concerning concrete structure cracks, which this study addresses.

One factor influencing concrete crack formation is tensile strength, which has a crucial role in controlling concrete cracking [5]. Concrete, characterized as a non-homogenous material composed of a binding medium and aggregated particles [6], inherently has unevenly distributed weak zones. These zones impact variations in mechanical properties, including its tensile strength, and its tendency to crack [5]. In instance of damage propagation, the variability of tensile strength often surpasses that of compressive strength [7]. This tensile strength is slightly correlated with structural size; larger structures tend to exhibit reduced tensile strength and increased material brittleness [8]. Concrete's natural variability and its nonlinear response to the applied forces can lead to situations where the maximum force exerted on the sample exceeds its tensile strength limit. This leads to a decreased ability of the concrete to resist initial cracking as the tensile force applied increases [1].

To measure tensile strength, laboratories conducted direct tensile tests by applying an axial load to concrete specimens through a steel bar casted within the samples until the specimens crack [9]. Various experimental works involving such tests have been conducted on concrete prism or beam samples, as performed by [10, 11, 12, 13]. In terms of concrete cracks, previous research has showed that even with identical samples and loading applications, the patterns and numbers of cracks generally vary, along with the distances between them. Despite these experimental insights, the inherent heterogeneity of concrete often remains unaddressed. Therefore, numerical simulations become essential, particularly in scenarios requiring high precision, such as the design of specialized structures like nuclear power plants and dams or in modelling concrete structure damage and cracking. Such simulations demand an exhaustive examination to understand the impact of heterogeneous characteristics on concrete's damage behaviour [1].

For the purpose of assessing the concrete's heterogeneity, the random field is utilized to capture the variability of its properties with The Turning Band Method (TBM) is employed to generate its random variables [14]. A previous numerical study that incorporated a random field in a concrete beam resulted in a noticeable crack localization compared to the sample without considering a random field, although it developed larger crack sizes [15]. Another study of random field which varying tensile strength and Young's modulus exhibited that the heterogeneity did not significantly affect the global behaviour, whereas the number of cracks in each sample remained consistent [16].

Moreover, earlier research applying The Turning Band Method (TBM) in concrete modelling [17], generated three distinct random field results, highlighting that TBM did not significantly alter the overall behaviour of the concrete beam. It emphasized diverse local crack patterns for each generated random field, respectively. Therefore, given due consideration, The Turning Band Method (TBM) application in concrete modelling is suitable to describe and point out the probability of damage patterns and crack phenomena.

In this study, acknowledging the heterogeneous nature of concrete, we aim to predict the probability of crack pattern of reinforced concrete with a single reinforcement bar. Turning Band Method (TBM) was employed to generate the random field by using a finite element software, Cast3M, specifically with the element CUB8, alongside the Mazars Damage Model to simulate concrete damage behaviour. To develop the random variables using TBM for concrete samples subjected to axial tensile load, the mesh size used in this simulation is 1 cm with a variety of correlation lengths is 1 cm, 2 cm, and 3 cm. Each correlation, ten random fields were generated. Furthermore, the crack patterns obtained from the computational analysis were compared to the samples of uniform strength and experimental samples to validate the modelling result against previous studies conducted by [11] and [17]. Comparisons were also made with simulations of random fields by [15] and [16].

The discussion section delves into the crack opening resulting from the application of the TBM, affirming its effectiveness on the modelled concrete material, which is indicative of the quality control of concrete casting. The discussion emphasizes the general behaviour (force vs displacement) that induces variations in the 1st crack localization, corroborated by the observed differences in damage occurrence across ten random field simulations. The first crack localization is critical, as it pertains to the concrete's serviceability and consequently, the structural performance under service conditions.

2.0 METHODOLOGY

In this section, a detailed numerical simulation methodology is presented. The specimen is configured as a simple beam with a single reinforcement cast inside a prismatic concrete beam. Numerical simulations involve subjecting the specimen to tension at one end of the bar whilst the other is fixed. This experimental setup is deliberately selected to facilitate an investigation into the behaviour of concrete under pure tensile loading conditions, aimed at observing and analysing crack initiation and propagation under the influence of pure tension loading. One-fourth of the sample is modelled, followed by the application of TBM and Mazars damage on concrete only. After obtaining a random draw, samples were charged in displacement-controlled conditions up to 8 mm. Thus, in this section, the Mazars model and TBM are explained, and followed by the simulation of the samples.

2.1 Theoretical Study

The focal point of this research lies in the adoption of the Mazars damage model and an in-depth examination of the specifics of the Turning Band Method (TBM). So, in this section, the theory of the Mazars Damage model and the Turning Band Method (TBM) is first described. Secondly, numerical simulations that are used to perform the proposed model are explained.

2.1.1 Mazars Damage Model

Damage is known as the conditions due to the cavity development at any level of microscopic, mesoscopic, and macroscopic, which describes a fracture process of materials that concurrently occurs with the reduction of mechanical properties. The damage aspects are varied depending on the material differences and the loading conditions [18]. Mazars developed an elastic isotropic damage model which can be applied to concrete material. As the damage model is isotropic, therefore, it only has 1 (one) scalar variable (D) that can be defined with a range of values between 0 and 1. The value of 0 demonstrates an un-damaged material (virgin state of material), while the damage value of 1 is expressed as a fully damaged condition. Moreover, there are parameters of damage for tension and compression that should be identified, such as At, Bt, Ac, and Bc [19]. A computational study using the Mazars Damage Model was done by [20] to model Oil Palm Shell (OPS) lightweight concrete in cube specimens, in which the parameters implementations showed a dependency on mesh density and size dimension.

2.1.2 Turning Band Method (TBM)

The Turning Band Method (TBM) was originally introduced by [21] as a means of simulating the realization of a random function. Serving as a generator, TBM facilitates the generation of a spatially correlated random variable in 2D and 3D through a complex 1D process, with its generation procedures and 2D visualizations detailed by [22]. The Turning Band Method (TBM) is one of the random field generators included in the Class 1 generator that produces a continuous random field using the point discretization method [14].

On the other hand, random fields are generally used to model uncertainty, such as an error in measurement, a random fluctuation of geometry or material properties, etc. In statistical analysis, random variables are used as a representation of uncertainty, therefore, rendering them suitable for the precise production of random fields [23]. A random field is affected by mesh density, in which in the generation process, mesh definition is required and related to the correlation function [14]. In line with that, it is assumed that the 2 (two) parameters, mesh size and correlation length may exert a notable influence on the modelling results. Thus, emphasizing the importance of meticulous consideration in their selection is necessary.

2.2 Numerical Simulation

The numerical study was conducted using the ALEA operator, an operator of The Turning Band Method (TBM) within the 2021 version of Cast3M, a finite element code-based application [24]. The behaviour of concrete law employed in this simulation is the Mazars Damage Model.

2.2.1 Proposed Model

The modelling is performed on a concrete beam which has a dimension of 100 x 100 x 500 mm^3 with a single reinforcement bar positioned at the centre of the concrete. However, to simplify the numerical simulation, only a quarter size of the sample is modelled in this modelling. The illustration of the proposed sample is shown in Figure 1.

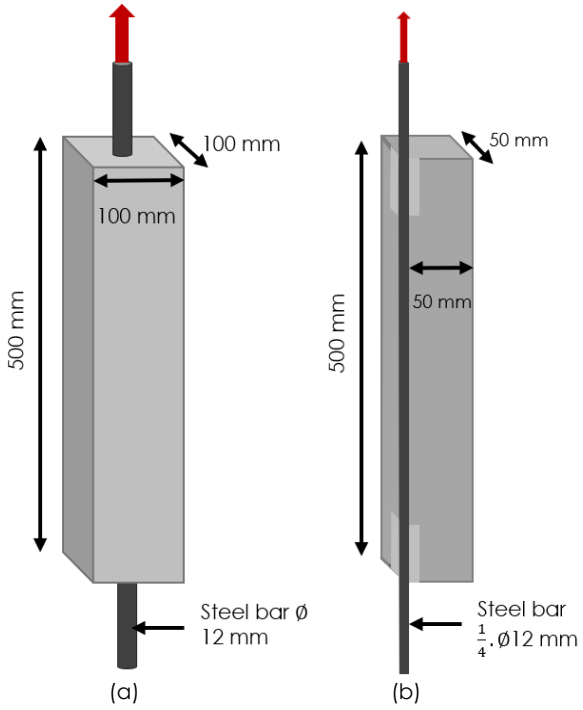

Figure 1 Proposed model of a reinforced concrete beam with single reinforcement bar (a) full size (b) ¼ of volume

2.2.2 Material Properties

The properties data of the reinforced concrete and the reinforcement bar in this simulation are based on the experimental works that have been done by [17]. The property of concrete materials is shown in Table 1.

Table 1 Mechanical Properties of Concrete

No.	Concrete Properties	Values
1	Specific Gravity (kg/m^3)	2400
2	Tensile Strength (MPa)	4 ± 0.2
3	Modulus of Elasticity (MPa)	38500
4	Poisson's ratio	0.27
5	Fracture Energy in Tensile (J/m^2)	154

The property of the reinforcement bar are shown below in Table 2.

Table 2 Reinforcement Bar Properties

No.	Reinforcement Properties	Values
1	Diameter of bar (mm)	12
2	Bar length (mm)	700
3	Yield Stress (MPa)	567.30
4	Elasticity Modulus (MPa)	190000

2.2.3 Size of Mesh and Length of Correlation

There are two main parameters that affect the random field, namely the mesh size and the length of correlation. The choice of mesh dimension in this modelling is directly related to the size of the coarse aggregate. In this numerical simulation, a mesh size of 1 cm is used, representing the minimum size of the aggregate. Whereas, the correlation length, also known as the fluctuation scale, denotes the range of variability within the random field. In cases involving concrete and reinforced concrete, the length of correlations is influenced by factors, such as mould designs and aggregate size, ultimately impacting the level of projection from the experimental data [14]. Given the pivotal role of the fluctuation scale in accurately characterizing variability, determining the precise value becomes crucial for achieving a realistic response in probabilistic approaches [25]. Consequently, the correlation length selection is dependent on the factor of aggregate size, which in turn affects the mesh size.

Therefore, in this modelling, the correlation length is set at 1, 2, and 3 times of the mesh dimensions with 10 times of random field generation for each length of correlation. These ten generated fields are taken to represent 10% of 100 experimental samples. Also, the modelling frequency must be carefully considered to ensure a failure pattern closely resembling the crack pattern of the laboratory-tested samples. Detailed information on the use of mesh dimensions, variations in correlation length, and modelling frequency is shown in Table 3.

Table 3 Mesh Size, Correlation Length Variation, and Frequency of Random Field

Mesh Size (cm)	Length of Correlation (cm)	Random Field Frequency (times)
1	1	10
	2	10
	3	10

2.2.4 Parameters of Mazars Damage Model

As stated before, the parameters of the Mazars Damage Model should be identified before the modelling is executed. The chosen parameters are obtained through a trial and error process, with the objection to achieving a global behaviour that closely aligns with the findings of the experimental study conducted by [17]. Each parameter of the Mazar damage model has a significant effect on the shape of the curve, and the illustration of their influence is described by [26]. Given that the test is performed under tension, only the parameters in tension, specifically At and Bt, are recognized. The specific values of these parameters employed in this modelling process can be found in Table 4.

Table 4 Mazar Damage Model Parameters

No.	Parameters	Values
1	At	0.95
2	Bt	9500
3	Shear Correction (β)	1.06

2.2.5 Boundary Conditions

The reinforced concrete beam with single reinforcement modelling is carried out on the ¼ size of the entire specimen. By using CUB8 elements, a 3D element which consists of 8 (eight) Gaussian integration points, a quarter size of the sample is detached based on their symmetrical axes. An interpretation of the CUB8 elements is shown in [27]. While the detailed information regarding the concrete and steel bar boundaries along with the tensile loading areas can be seen in Figure 2.

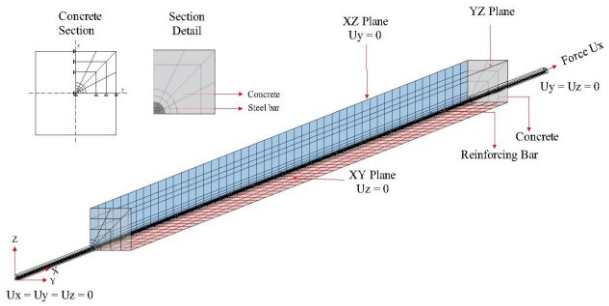

Figure 2 Boundary conditions of ¼ size of the concrete beam with single reinforcement bar

Based on Figure 1, the boundary conditions of concrete beams with single reinforcing bars are marked by different colours on each side of the sample. The side which has a blue colour indicates that the concrete is fixed in the Y direction, thereby prohibiting movement in that direction. On the other hand, the red colour signifies that concrete is fixed in the Z direction, resulting in actions occurring solely in the X and Y directions. The grey colour denotes that actions are primarily taking place in the X direction. Moreover, a tensile force is applied to one side of the end of reinforcing steel, while the other side of the bar

is restrained. This load is applied in the X direction until the concrete sample is damaged.

3.0 RESULTS AND DISCUSSION

This section discusses the analysis of numerical simulation results, which consists of the random draws, a force-displacement relationship that represents the global behaviour of concrete, damage behaviour, and tensile strength average value of each random field that has been generated towards the variation of the correlation length. The observation of the damage patterns is pointed out at the end of tensile loading.

3.1 Random draw from The Turning Band Method (TBM) implementation

By implementing the same mesh dimension and various lengths of correlation in the reinforced concrete beam modelling, random draws of all random fields were captured. The results are shown in Table 5 which describes the random draw from each random field alongside their length of correlation. As mentioned in Table 3, 30 random draws have been generated in this modelling which consists of 10 random draws that are produced by each correlation length (Lc).

Regarding Table 5, the random draws reveal the distribution of average tensile strength that illustrates its variability across different areas of the concrete sample. The scale of the colour is given on top of the table signifying the strength variation performed for the concrete volume. The colours in random draw signify specific conditions; the green colour indicates concrete areas which dominated by average tensile strength, the blue colour points out the areas with the lowest average tensile strength, and the orange colour specifies areas with the highest average tensile strength.

Table 5 Random draw results of concrete tensile strength using ALEA Operator in Cast3M with a variation of the correlation lengths

Random Field (RF)	Length of Correlation (cm)		
	1	2	3
	Tensile Strength (MPa)		
1	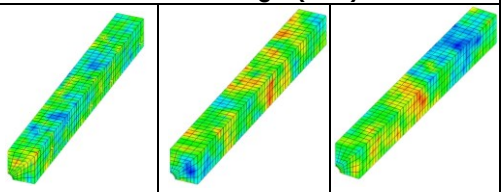		
2	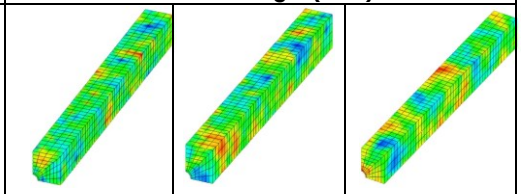		
3	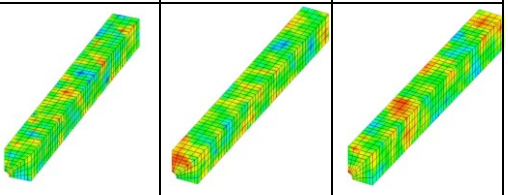		
4	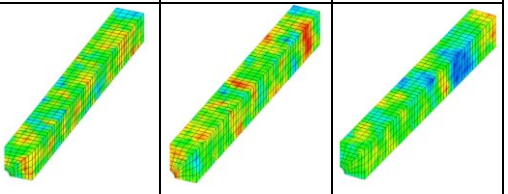		
5	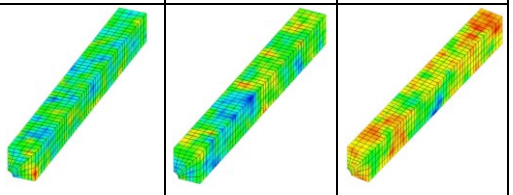		
6	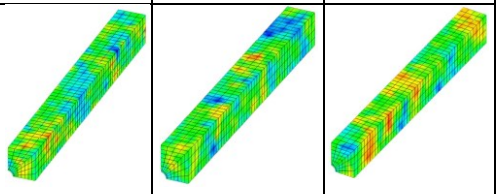		
7	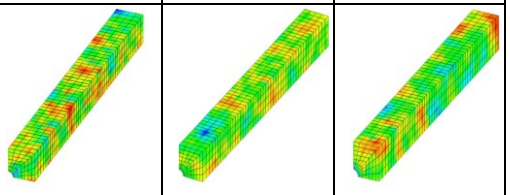		

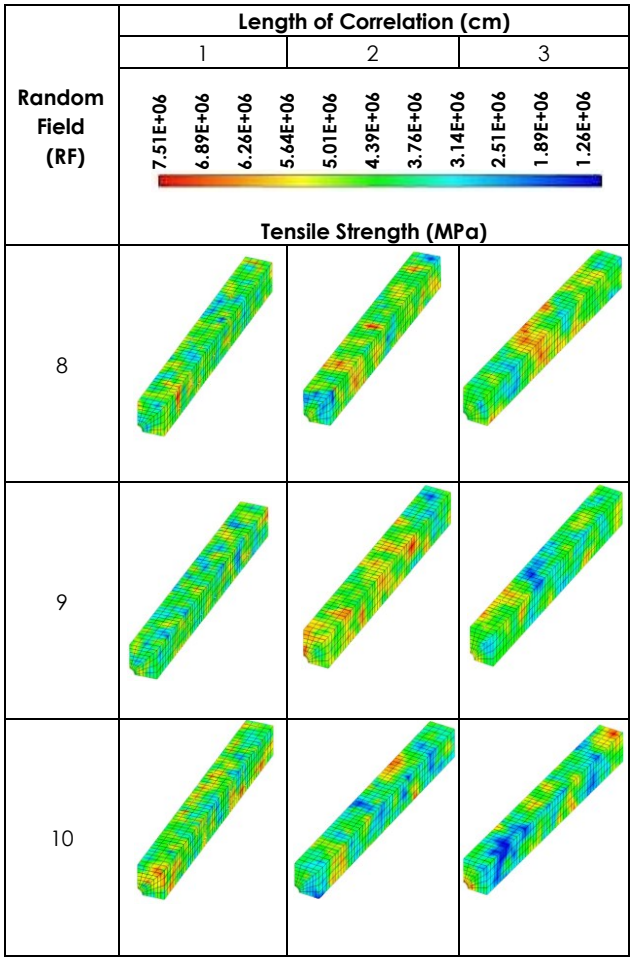

A noticeable effect caused by the adoption of correlation length is shown. Each random field depicts a distinct random draw, with the location of the lowest and highest values of average tensile strength is varied. Because of its role as the variability measurement, the length of correlation affects the distribution level of the mechanical properties, in this case, it is impacting the mean value of tensile strength that may not give the same value to every random field. In addition, the random draws generated using 1 cm of correlation length exhibit a coarser distribution of average tensile strength compared to those random draws generated using 2 cm and 3 cm.

To check the relevance to the input variables of the modelling, in this term, the tensile strength value acquired from the experimental test, the average value of the tensile strength of each random field obtained from the TBM simulation were calculated in Cast3M. The comparison of tensile strength average value between numerical simulation and laboratory test samples is shown in Figure 3.

Figure 3 shows the average tensile strength from simulations with the same mesh dimension and three types of correlation lengths. Tensile Strength of 4 MPa with 0.2 MPa of standard deviation was used (see Table 1 the concrete properties). In Figure 3, the purple shadow zone represents the standard deviation. Lc means correlation length. The results demonstrate that using different correlation lengths can lead to greater deviations in the average tensile strength values across each random field, specifically three cases for Lc equals 2 and 3 cm.

As shown in the curve, when using a 1 cm correlation length, the average tensile strength values derived from 10 generated random fields range between 3.90 MPa and 4.31 MPa (within the area of purple shadow). Conversely, at correlation lengths of 2 cm and 3 cm, the variation in tensile strength values across each random field is notably large, particularly in RF6 and RF7. Three random fields drawn from LC of 2 and 3 cm passed the standard deviation. Overall, the average tensile strength derived from all modelling samples ranged from 3.30 MPa to 4.30 MPa. The larger the Lc is, the larger the deviation is.

3.2 Global Behaviour: Force-displacement and First Crack(S) Localization

After obtaining random draws, the sample was then modelled under displacement control reaching 8 mm. The simulations resulted in 30 different force-displacement responses from 30 random draws. These responses are commonly known as global behaviour. Figures 4, 5, and 6 show the global behaviour from 10 random fields (named RF 1 until 10) of correlation lengths of 1 cm, 2 cm, and 3 cm. Each case is accompanied by non-TBM results (depicted in red colour).

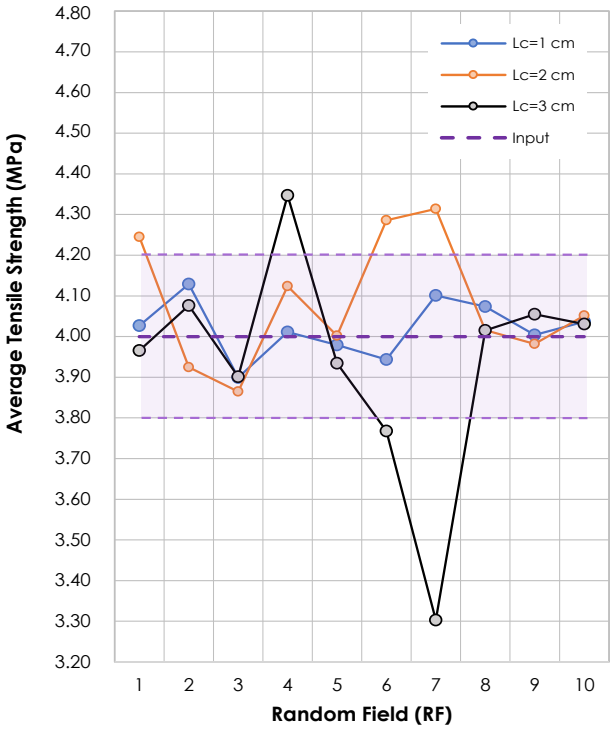

Figure 3 Average Tensile Strength of Simulation with The Turning Band Method (TBM) and Experimental Study

Regarding these three figures, a linear relationship between force and displacement is apparent in the beginning. It is possible due to steel reinforcement bar linear behaviour. Then, it changes little by little nonlinear as concrete damages. When damage localizes as first crack localization, the force decreases suddenly. It increases again along with the tension load and fall again to second crack localization. This condition occurs until yielding condition reached. For some cases occurs only one dropped force (localized damage), for the other cases occur 2 to 3 times.

Therefore, for each case of Lc, Turning Band Method (TBM), in general, does not significantly influence the global behaviour (force-displacement relationship) of each generated random field. On the other hand, the first crack localization is. All random fields exhibit several points of crack localization at different loading rates both before and after reaching the elastic limit. Meanwhile, the modelling without Turning Band Method (non-TBM) indicates that the one localization of concrete crack only occurs before achieving the elastic limit.

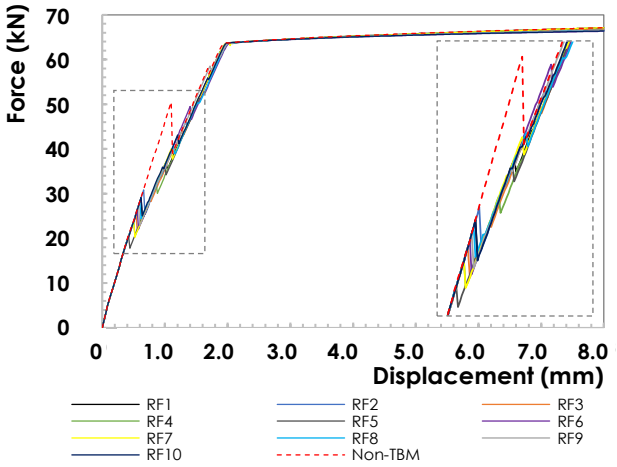

Figure 4 Graph of Force - Displacement for numerical simulation using TBM with 1 cm of correlation length and modelling without The Turning Band Method (TBM)

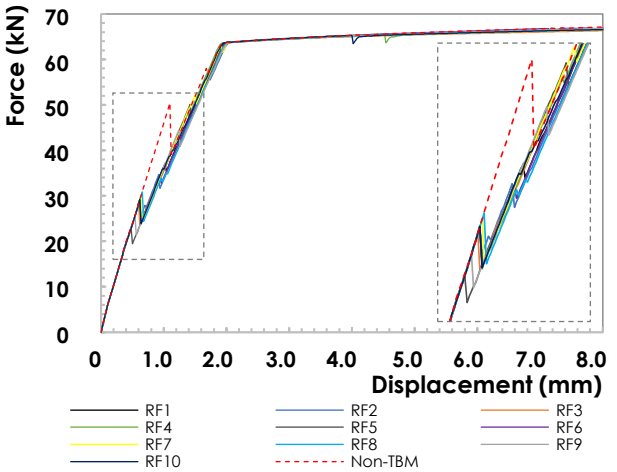

Figure 5 Graph of Force - Displacement for numerical simulation using TBM with 2 cm of correlation length and modelling without The Turning Band Method (TBM)

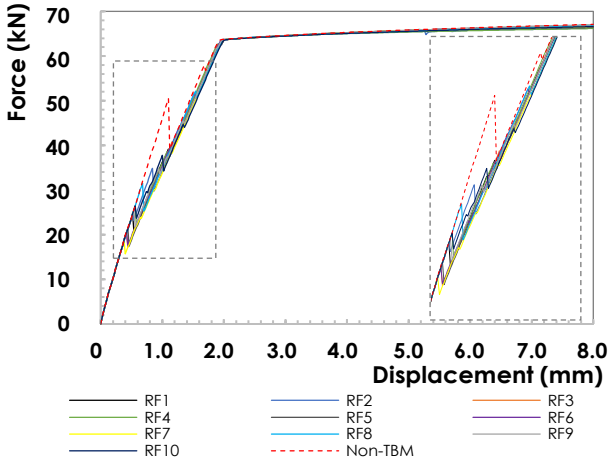

Figure 6 Graph of Force - Displacement for numerical simulation using TBM with 3 cm of correlation length and modelling without The Turning Band Method (TBM)

Table 6 describes the summary of the first crack(s) localization for each case. For the case of non-TBM modelling, the first crack localization occurred at 50.5 kN. On the other hand, for the TBM modelling, the first crack can occur within the range of 18.70 kN to 31.50 kN. Thus, crack localization obtained from The Turning Band Method (TBM) simulations can take place earlier than the modelling of non-TBM.

In terms of the displacement at the first crack(s) localization in both cases of TBM and non-TBM also differs. In the non-TBM case, the displacement estimates at force of 50.5 kN is 1.10 mm. While, in the case of TBM implementation by using different lengths of correlation of 1, 2, and 3 cm causes displacements ranging between 0.42 mm to 0.62 mm in the conditions of first crack localization. Accordingly, the displacement at the first localization of the crack of non-TBM sample is larger than TBM samples.

Table 6 Force and displacement just before the First Crack(s) localization

Non-Random Field	$F = 5.05\times10^{04}$ N d = 1.10 mm		
Correlation Length / **Random Field**	**1 cm**	**2 cm**	**3 cm**
1	$F = 2.91\times10^{04}$ N d = 0.62 mm	$F = 2.73\times10^{04}$ N d = 0.58 mm	$F = 2.47\times10^{04}$ N d = 0.52 mm
2	$F = 3.09\times10^{04}$ N d = 0.66 mm	$F = 2.92\times10^{04}$ N d = 0.62 mm	$F = 2.48\times10^{04}$ N d = 0.52 mm
3	$F = 2.56\times10^{04}$ N d = 0.54 mm	$F = 2.84\times10^{04}$ N d = 0.60 mm	$F = 2.04\times10^{04}$ N d = 0.42 mm
4	$F = 2.38\times10^{04}$ N d = 0.50 mm	$F = 2.92\times10^{04}$ N d = 0.62 mm	$F = 2.04\times10^{04}$ N d = 0.42 mm
5	$F = 2.05\times10^{04}$ N d = 0.42 mm	$F = 2.28\times10^{04}$ N d = 0.48 mm	$F = 2.14\times10^{04}$ N d = 0.44 mm
6	$F = 2.64\times10^{04}$ N d = 0.56 mm	$F = 2.91\times10^{04}$ N d = 0.62 mm	$F = 2.04\times10^{04}$ N d = 0.42 mm
7	$F = 2.37\times10^{04}$ N d = 0.50mm	$F = 3.01\times10^{04}$ N d = 0.64 mm	$F = 1.87\times10^{04}$ N d = 0.38 mm

Non-Random Field	F = 5.05×10^{04} N d = 1.10 mm		
Correlation Length	**1 cm**	**2 cm**	**3 cm**
8	F = 2.82×10^{04} N d = 0.60 mm	F = 3.09×10^{04} N d = 0.66 mm	F = 3.15×10^{04} N d = 0.68 mm
9	F = 2.75×10^{04} N d = 0.60 mm	F = 2.55×10^{04} N d = 0.54 mm	F = 2.54×10^{04} N d = 0.54 mm
10	F = 2.91×10^{04} N d = 0.62 mm	F = 2.92×10^{04} N d = 0.62 mm	F = 2.65×10^{04} N d = 0.56 mm

Regarding Table 6, Figures 7 and 8 depict the box plot of the peak force and the corresponding displacement just before the first crack localization from the three cases of Lc. In these figures, red stripes represent the average value before the first crack localization, and the rest statistical values are as noted in Figure 7. It can be said that Lc 3 has the largest standard deviations, either for the force or for the corresponding displacement among all, while Lc 2 has the lowest one. Comparing to the results from section 3.1, Figure 8 shows that Lc 3 cm has the largest deviation, aligned with first crack localization displacement and force. On the other hand, it is not the case with the Lc 1 cm and 2 cm. So, the standard deviation of tensile strength from the generated random draws is not related directly to the variation of first crack localization. Nevertheless, the longest Lc has largest variation.

In this simulation, the impact of TBM applications leads to earlier cracking, as observed in both force and displacement. In real condition, if first crack can be predicted earlier, it can help engineers preventing further loss.

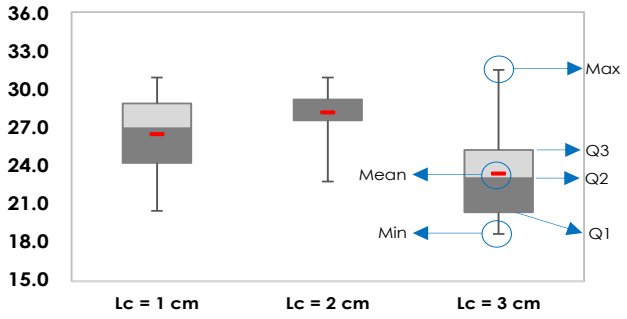

Figure 7 Box Plot of Peak Force just before the first crack(s) localization

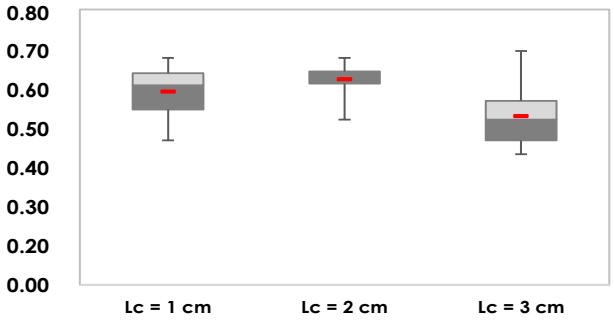

Figure 8 Box Plot of Displacement of Peak Force just before the first crack(s) localization

3.3 Damaged Condition at the End of the Test

The damage pattern of each random field of concrete prism samples for every correlation length can be seen in Table 7. The cracks of each random field are observed at the end of tensile loading, highlighting the point of maximum tensile force at 8 mm of displacement. The range values for the maximum tensile loading utilized to assess the crack conditions across all random fields fall approximately between 6.62 x 10^4 N and 6.71 x 10^4 N.

Each correlation length results an unconventional crack pattern, which is characterized by varied locations and quantities of cracks. Damage colours indicate different conditions; the appearance of red colour on the concrete surface denotes regions that have incurred damage, whereas the blue colour represents that the concrete areas have negligible damage. The scale of the damage is presented on top of the table.

Table 7 Damage pattern of each random field with a different correlation length

Random Field (RF)	Length of Correlation (cm)		
	1	2	3
	0.930 0.840 0.750 0.660 0.570 0.480 0.390 0.300 0.210 0.120 0.003		
1	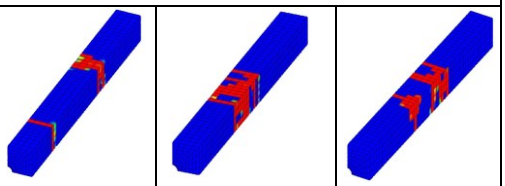		
2	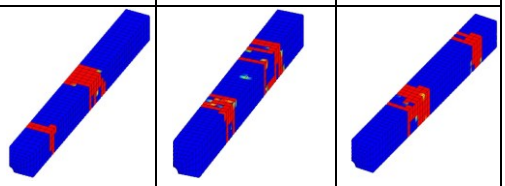		
3	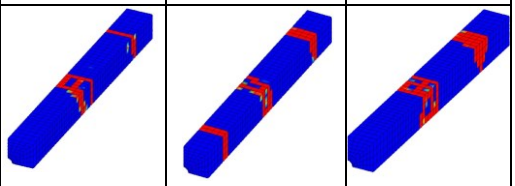		
4	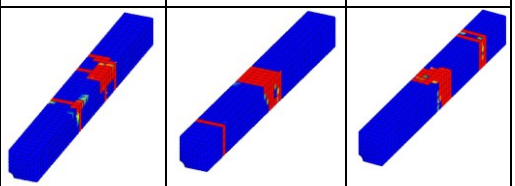		

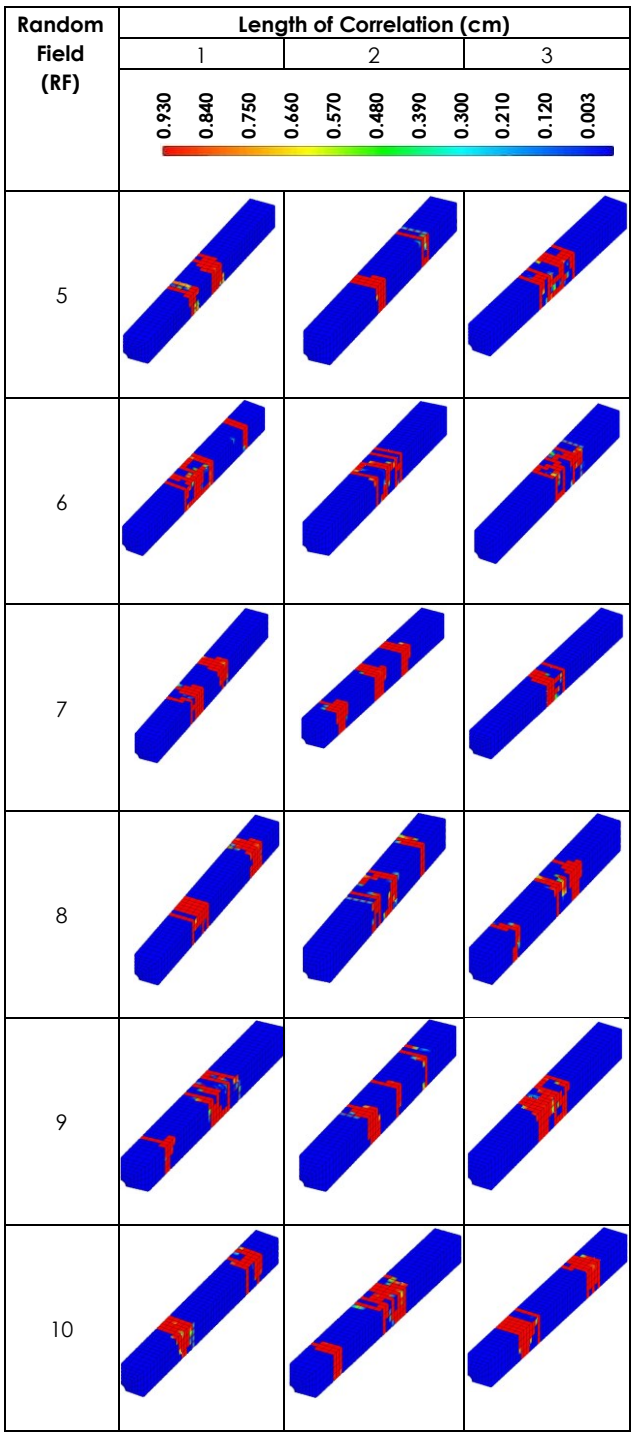

It is observed that each random field has different number of cracks, in which by generating the random field using a correlation length of 1 cm, it generally exhibits 2 cracks, while the utilization of larger correlation lengths, specifically 2 cm and 3 cm, results in a range of 1 to 3 cracks. The first cracks typically appear in the middle length of the concrete samples, and the number of cracks may rise and propagate with the increasing tensile force.

The observed damage patterns are linked to the outcomes of each random draw across different random fields, as shown in Table 5. Initial cracks predominantly form in areas identified as weak zones, characterized by the lowest average tensile strength within the concrete. Consequently, the location and number of cracks vary across each random field, highlighting these regions' increased vulnerability to cracking compared to other concrete areas. Additionally, as demonstrated in Table 6, initial cracks are typically found at the mid-span of the concrete sample. From this point origin, the cracks tend to propagate or expand to adjacent areas throughout the tensile loading process.

The crack patterns obtained from the modelling with TBM, as displayed in Table 7, are compared with those from a numerical simulation non-TBM, using identical Mazars Damage Model parameters. Figure 9 denotes that non-TBM modelling of concrete samples results in a single crack, located at the mid-length of the concrete sample. Beyond the initial crack, no additional crack development is observed until the end of the loading; but only the widening of damage is occurred.

The damage patterns presented in Table 7 are compared with the experimental results reported by [17]. The prior study involved the tensile testing of two single reinforced concrete samples, labelled as ER1 and ER2. Laboratory finding revealed that the ER1 sample exhibited 2 cracks on its mid-surface, whereas the ER2 sample showed a singular crack, remaining in a fixed position throughout the loading duration.

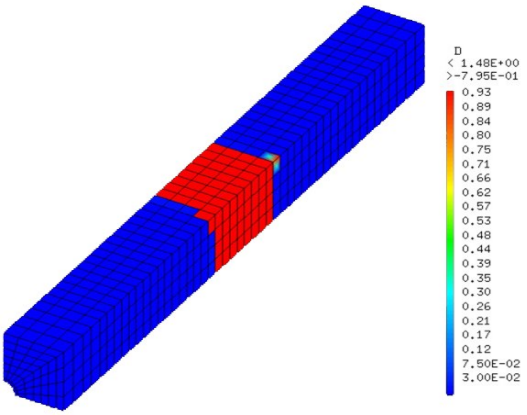

Figure 9 Damage Pattern of Modelling without TBM

The comparison of crack numbers between experimental samples [17] and models incorporating TBM, to consider the heterogeneity nature of concrete, shows that models with a 2 cm correlation length generally yield more cracks than observed in laboratory tests. Models with a 1 cm correlation length tend to resemble the damage pattern of the ER1 sample, whereas models using a 3 cm correlation length align more closely with the ER2 test results.

The results were further compared with experimental work conducted by [11] on beams

measuring 10 x 10 x 100 cm^3. These three specimens exhibited 5 to 6 cracks, localized at the end of the tensile loading, with crack positions perpendicular to the loading axis at the end of each beam. Compared to the numerical simulation employed TBM, it showed that the experimental study revealed a higher crack count. Additionally, it showed that cracks were positioned closely along the tie beam, whereas the TBM simulations indicated that some results had more widely spaced cracks.

The modelling outcomes were analysed alongside the random field simulation performed by [15], which aimed to predict cracking in both plain and steel fibre-reinforced concrete using the Hordijk model and a smeared crack approach in DIANA. This comparison showed an agreement in findings, highlighting that the random field model resulted in varying crack widths and spacing due to crack localization, with steel fibre contributing to reduced crack width.

When compared with the random field modelling completed by [16], which employed a steel-concrete bond model in the same finite element code Cast3M, similar levels of agreement were observed. This study indicated that while the global responses remained largely unaffected by the 3 random field generations, the localization of the first crack, particularly in relation to peak load, differed. At a local level, the crack opening demonstrated consistency in the number, with five cracks observed at the end of loading with small space. Nevertheless, the specific crack patterns across each random field exhibited significant variability.

4.0 CONCLUSION

In conclusion, the utilization of The Turning Band Method (TBM) has significantly impacted the simulation of concrete with a single reinforcement bar. Employing the same mesh size and varying correlation length revealed that the global behaviour, as indicated by the force–displacement relationship, experienced a negligible change due to these parameters. However, it demonstrated varying frequencies of tensile force instability in each random field, highlighting the occurrence of first crack(s) localization at different forces (and displacement).

The use of different correlation lengths resulted in diverse crack patterns, with each random field exhibiting different crack positions and quantities. Initial cracks primarily emerged in the middle surface of the concrete samples, with certain random fields showing an increase in crack quantity with the increasing applied force.

A comparison between modelling TBM and non-TBM revealed that the TBM modelling demonstrated a diverse crack pattern, whereas the non-TBM samples exhibited a single crack at the centre. Comparison with the experimental results showed that the random field modelled using a 1 cm correlation length exhibited a crack pattern similar to ER1, while the simulation using a 3 cm correlation length exhibited a crack pattern akin to sample ER2. Moreover, the smaller correlation length exhibited only a slight deviation from the experimental study, while the larger correlation length demonstrated a considerable deviation in tensile strength.

For ten random field simulations for each correlation length, crack modelling on concrete structures may result in different crack openings. In the case of experimental works, cracks occur differently for the same condition of concrete. Thus, TBM may help to represent crack simulations for real applications that need detailed crack propagation locations along the concrete volume.

In brief, the findings revealed that TBM enables more accurate and realistic concrete modelling by accounting for the heterogeneous nature of concrete. This method yields results that closely align with experimental results. The fact that TBM model can predict earlier damage in concrete may help engineers for reducing loss due to more severe damages.

Future research should explore the possibility of other concrete properties, such as shrinkage and aggregate size distribution, to enhance understanding of concrete modelling. Further examination of concrete damage in more intricate structural elements, such as beams with complex reinforcement configurations, represents a promising direction for subsequent research.

Acknowledgements

This research is supported by Structural and Material Laboratory Department of Civil Engineering, Faculty of Engineering, Universitas Indonesia.

Conflicts of Interest

The author(s) declare(s) that there is no conflict of interest regarding the publication of this paper.

References

[1] Francis Barre, Philippe Bisch, Danièle Chauvel, Jacques Cortade, Jean-François Coste, Jean-Philippe Dubois, Silvano Erlicher, Etienne Gallitre, Pierre Labbé, Jacky Mazars, Claude Rospars, Alain Sellier, Jean-Michel Torrenti, François Toutlemonde. 2016. *Control of Cracking in Reinforced Concrete Structures Research Project CEOS.fr*. John Wiley & Sons, Inc.

[2] S. Shahidan, S. R. Abdullah, and I. Ismail. 2015. Relationship Between AE Signal Strength and Absolute Energy in Determining Damage Classification of Concrete Structures. *J. Teknol.* 78(5): 1-8. Doi: https://doi.org/10.11113/jt.v78.8248.

[3] N. H. Suliman, A. A. Bakar, S. H. Hamzah, and N. A. Ahmad. 2015. Crack Behaviour of Pre-Tensioned (PRT) Concrete Beam after Retrofitted with CFRP Sheets. *J. Teknol.* 76(9): 1-4.

Doi: https://doi.org/10.11113/jt.v76.5686.
[4] Q. M. Shakir and B. B. Abd. 2020. Retrofitting of Self-compacting RC Half Joints with Internal Deficiencies by CFRP Fabrics. J. *Teknol.* 82(6): 49-62. Doi: https://doi.org/10.11113/jurnalteknologi.v82.14416.
[5] Maria Ghannoum. 2018. Effects of Heterogeneity of Concrete on the Mechanical Behavior of Structures at Different Scales. Materials. Université Grenoble Alpes. English. NNT: 2017GREAI035. https://tel.archives-ouvertes.fr/tel-01721630.
[6] Z. Li. 2011. *Advanced Concrete Technology*. New Jersey: John Wiley & Sons, Inc.
[7] Badan Standarisasi Nasional Indonesia. 2013. SNI 2847:2013, Persyaratan Beton Struktural untuk Bangunan Gedung. Bandung Badan Stand. Indonesia. 1-265.
[8] X. Du and L. Jin. 2021. Size Effect in Concrete Materials and Structures. Doi: https://doi.org/10.1007/978-981-33-4943-8.
[9] R. Madandoust, M. Kazemi, and S. Y. Moghadam. 2017. Study on Tensile Strength of Concrete. *Rom. J. Mater.* January: 294-297.
[10] Y. Goto and K. Otsuka. 1980. Experimental Studies on Cracks Formed in Concrete around Deformed Tension Bars. *Proc. Japan Soc. Civ. Eng.* 294: 85-100. Doi: https://doi.org/10.2208/jscej1969.1980.294_85.
[11] A. Michou, A. Hilaire, F. Benboudjema, G. Nahas, P. Wyniecki, and Y. Berthaud. 2015. Reinforcement-concrete Bond Behaviour: Experimentation in Drying Conditions and Meso-scale Modeling. *Eng. Struct.* 101: 570-582. DOI: https://doi.org/10.1016/j.engstruct.2015.07.028
[12] H. Q. Wu. 2010. Tension Stiffening in Reinforced Concrete - Instantaneous and Time-Dependent Behaviour. 348. unsworks.unsw.edu.au/fapi/datastream/unsworks:8336/SOURCE02%5Cn.
[13] N. Handika, G. Casaux-Ginestet, and A. Sellier. 2015. Influence of Interface Zone Behaviour in Reinforced Concrete under Tension Loading: An Analysis based on Modelling and Digital Image Correlation. *Proc. 8th Int. Conf. Comput. Plast. - Fundam. Appl. COMPLAS 2015*. 122-133.
[14] R. Van der Have, 2015. Random Fields for Non-Linear Finite Element Analysis of Reinforced Concrete. November: 244. http://repository.tudelft.nl/islandora/object/uuid:25780e9a-49c4-4085-9a65-af73119d97a7?collection=education.
[15] A. van den Bos and A. Garofano. 2017. Crack Predictions using Random Field. Crack width Calc. Methods Large Concr. Struct. Work. *Proc. from a Nord. Miniseminar.* 12(November 2016): 87-94.
[16] C. Mang. 2016. Modeling of Steel-Concrete Bonds in the Calculation of Reinforced Concrete Structures. Nuclear Energy Department, Nuclear Activities Department of Saclay, CEA Saclay.
[17] N. Handika. 2017. Multi-cracking of Reinforced Concrete Structures: Image Correlation Analysis and Modelling. *Civil Engineering*. INSA de Toulouse.
[18] S. Murakami. 1967. *Continuum Damage Mechanics*. 185(1): 69. Morikita Publishing Co. Ltd., Tokyo.
[19] G. Pijaudier-cabot, J. Mazars, G. Pijaudier-cabot, J. Mazars, D. Models, and J. Lemaitre. 2017. *Damage Models for Concrete*. 500-512. Doi: https://doi.org/10.1016/B978-012443341-0/50056-9.
[20] K. Hongsen, M. Melhan, N. Handika, and B. O. B. Sentosa. 2021. Parameterization of Oil Palm Shell Concrete on Numerical Damage Model Based on Laboratory Experiment using Digital Image Correlation. *J. Phys. Conf. Ser.* 1858(1): 202. Doi: https://doi.org/10.1088/1742-6596/1858/1/012029.
[21] G. Matheron. 1973. Intrinsic Random Functions and Their Applications. *Adv. Appl. Probab.* 5(3): 439-468. Doi: https://doi.org/10.1017/S0001867800039379.
[22] G. A. Fenton. 1994. Error Evaluation of Three Random-Field Generators. *J. Eng. Mech.* 120(12): 2478-2497. Doi: https://doi.org/10.1061/(ASCE)0733-9399(1994)120:12(2478)
[23] Y. Liu, J. Li, S. Sun, and B. Yu. 2019. Advances in Gaussian Random Field Generation: A Review. *Comput. Geosci.* 23(5): 1011-1047. Doi: https://doi.org/10.1007/s10596-019-09867-y.
[24] Cast3M. http://www-cast3m.cea.fr/. Accessed Apr. 29, 2023.
[25] M. Lloret-Cabot, G. A. Fenton, and M. A. Hicks. 2014. On the Estimation of Scale of Fluctuation in Geostatistics. *Georisk Assess. Manag. Risk Eng. Syst. Geohazards*. 8(2): 129-140. Doi: https://doi.org/10.1080/17499518.2013.871189.
[26] Code-Aster v14 0.1 documentation. 15. R7 : Material models. 15.1. [R7.01.08]: MAZARS Damage Model for Concrete. https://biba1632.gitlab.io/code-aster-manuals/docs/reference/r7.01.08.html. Accessed Dec. 10th, 2023.
[27] E. Le Fichoux. 2011. *Annotated Testing Files*. 420.